

Absorption and Hot-Electron Production for 1.05 and 0.53 μm Light on Spherical Targets

D. C. Slater, Gar. E. Busch, G. Charatis, R. R. Johnson, F. J. Mayer, R. J. Schroeder,
J. D. Simpson, D. Sullivan, J. A. Tarvin, and C. E. Thomas

KMS Fusion, Inc., Ann Arbor, Michigan 48106

(Received 8 December 1980)

Laser-plasma interaction experiments have been performed with both 1.05- and 0.53- μm -wavelength light incident on spherical glass targets. Comparisons of hard x-ray spectra and fast-ion energy imply a substantial reduction of hot-electron levels at the shorter wavelength. Increased absorbed energy fractions at the shorter wavelength are in agreement with the expected scaling of inverse bremsstrahlung absorption.

PACS numbers: 52.25.Ps, 52.40.Db, 52.50.Jm

The interaction of high-intensity laser light with dense plasma has been studied extensively with high-power, short-pulse Nd:glass lasers operating at wavelengths near 1 μm . In the target irradiance regime from 10^{14} to 10^{16} W/cm^2 that is of interest to laser fusion, a number of plasma processes have been observed that are detrimental to the goal of achieving net energy release with the smallest possible laser energy input. In the underdense plasma stimulated Brillouin scattering can prevent light from reaching the absorption region.¹ Resonance absorption, which is an important absorption mechanism, generates penetrating hot electrons at the critical density surface.^{2,3} These and other problems have fostered interest in the use of shorter wavelength laser light that offers substantial improvements based on our present understanding of wavelength scaling. In general, nonlinear interaction processes increase as the ratio $(v_0/v_e)^2$ increases, where v_0 is the electron oscillatory velocity in the electromagnetic field and v_e is the electron thermal velocity. This ratio is proportional to $I\lambda^2/T_e$, where I and λ are the laser intensity and wavelength and T_e is the electron temperature. The *a priori* expectation is that for shorter wavelength light the plasma will exhibit less collective behavior. Max and Estabrook have recently reviewed wavelength scaling for a wide variety of processes related to laser fusion, and they conclude that strong benefits exist at wavelengths considerably less than 1 μm .⁴ Absorption measurements at 0.53 μm have been made on a variety of planar targets⁵⁻⁷ and on spherical glass-shell targets.⁸ Hot-electron temperatures have been measured on planar CH targets.⁶

The experiments presented here provide data on hot-electron production and energy absorption at 1.05 and 0.53 μm . Target parameters, laser pulse parameters, and focusing optics were care-

fully matched to facilitate detailed comparisons at the two wavelengths. Data were taken in two pulse-length regimes, 80–100 and 350–500 psec, and over a range of irradiance levels, from 6×10^{14} to 1×10^{16} W/cm^2 . The targets were spherical glass shells filled with approximately 2 mg/cm^3 of DT gas. Most of the targets had diameters in the range from 75 to 89 μm . Smaller-diameter targets (52 to 59 μm) were used on about 20% of the shots to reach the highest desired irradiances. The target wall thicknesses for all of the longer pulse shots were in the range from 4 to 6 μm . For the short pulse shots the target wall thicknesses were in the range from 0.9 to 1.2 μm . These wall thicknesses were chosen so that the target collapse time would be approximately equal to the laser pulse length.

The CHROMA I laser system at KMS Fusion is a Nd:glass laser operating at 1.053 μm . The oscillator produces a single pulse with full width at half maximum of 80 to 100 psec. The longer pulses were obtained by combining four or five single pulses. Laser light was converted to the second harmonic by 14-cm type-II potassium dihydrogen phosphate crystals. Beam quality was quite similar at the two wavelengths. At the target-equivalent focal plane the peak-to-average intensity variation was 2.5 ± 0.8 at 1.05 μm and 2.5 ± 0.5 at 0.53 μm . Minimum focal-spot diameters for 90% enclosed energy were 9.2 ± 2.9 μm in the infrared and 15.5 ± 2.8 μm in the green. The target illumination optical system consists of two lens-ellipsoidal-mirror pairs which provide nearly uniform illumination on spherical targets.⁹

The temperature of hot electrons produced by resonance absorption is expected to scale as $(I\lambda^2)^\delta$, where $\delta = 0.3$ to 0.4 .^{2,3} Lower hot-electron temperatures are preferred for laser fusion because the penetration depth of hot electrons into the target is proportional to the square of the

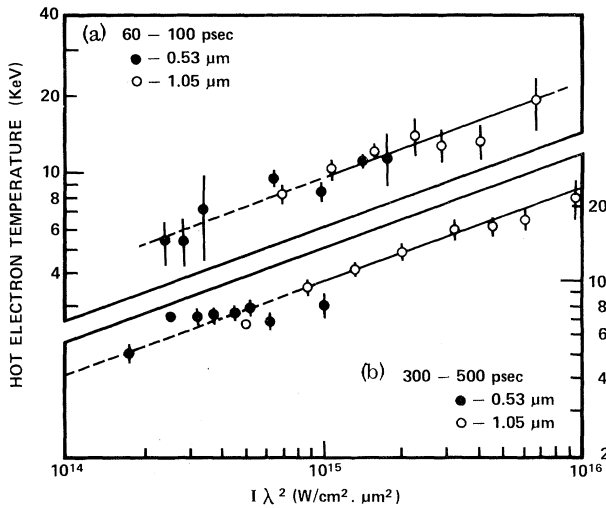


FIG. 1. Hot-electron temperature from x-ray continuum spectrum for (a) shorter pulse length and (b) longer pulse length.

temperature. Hot-electron temperatures are deduced from the slope of hard x-ray spectra measured with an array of nine *p-i-n* diodes with various *K*-edge filters in the range from 4 to 40 keV. All of the spectra could be reasonably well fitted with a two-temperature bremsstrahlung model. The higher temperature component is plotted in Fig. 1. The incident irradiance is taken to be the incident laser energy divided by the pulse length (full width at half maximum), divided by the target surface area. Each datum point is the average over a group of three to ten shots with similar irradiance levels, weighted by a goodness-of-fit parameter from the spectrum fitting routine. The error bars indicate one standard deviation from the group average and do not include any estimate of systematic error. The solid line on the figure represents the best fit to data obtained at 1.06 μm on glass-shell targets at the Lawrence Livermore National Laboratory.¹⁰ The slope of this line is $\delta = 0.39$, in good agreement with resonance absorption theory and CH target data.⁶

Other indications of reduced hot-electron levels are obtained by comparing the total energy in the hard x-ray spectrum and the total fast-ion energy at the two wavelengths. Figure 2(a) shows the fraction of the absorbed energy in the hard x-ray spectrum, obtained by extrapolating the high-temperature x-ray component to zero x-ray energy and integrating to obtain the total energy. The comparison of 1.05- and 0.53- μm data suggests approximately a fourfold reduction in supra-

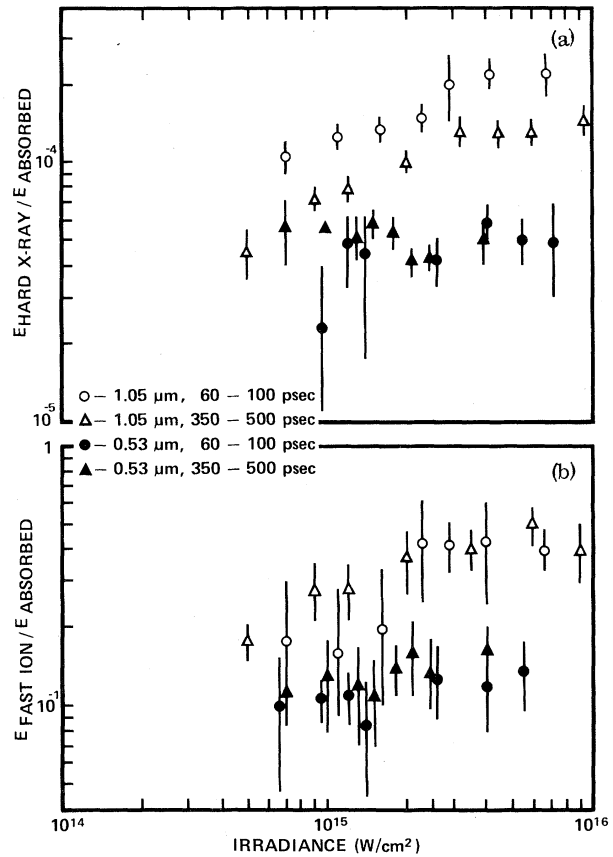


FIG. 2. (a) Total hard x-ray energy fraction and (b) total fast-ion energy fraction vs laser irradiance. Error bars are statistical only and do not include calibration uncertainty.

thermal energy in the latter. A similar reduction in the total energy carried by fast ($> 10^8$ cm/sec) ions is evident in Fig. 2(b). The fast-ion data are from charge collectors that were calibrated at 1.05 μm for charge-to-mass ratio and secondary electron emission. They are supported by Thomson parabola ion spectra recorded on cellulose-nitrate foils. The wavelength comparison again shows substantial reduction of suprathermal energy at 0.53 μm . The reduction in the energy carried away from the target in the form of fast ions implies substantially increased momentum transfer to the target and hence increased implosion efficiency for the shorter-wavelength incident light. The only significant pulse-length dependence in Fig. 2 is in the 1.05- μm hard x-ray data. The hard x-ray fraction is reduced by a factor of 1.4 for the longer pulses.

The absorbed energy was determined with a dif-

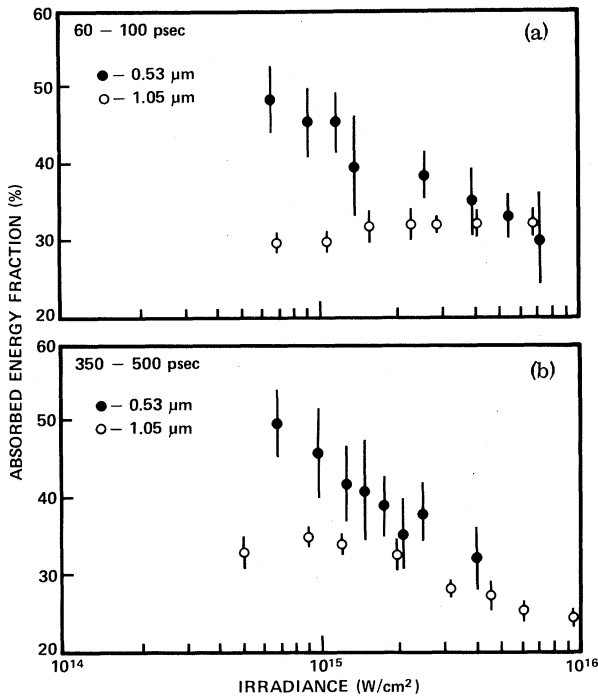


FIG. 3. Absorbed energy fractions vs laser irradiance for (a) shorter pulse length and (b) longer pulse length.

ferential plasma calorimeter mounted toward the top of the vacuum chamber away from the target mounting stalk. Measured absorbed energy fractions are shown in Fig. 3. The results are averages of several shots with nearly identical target and incident pulse parameters. At both pulse lengths the 0.53 μm absorption is substantially greater at the lower irradiances and decreases with increased irradiance. This scaling is characteristic of inverse bremsstrahlung absorption. The 1.05 μm absorption is much less sensitive to irradiance as would be expected for resonance absorption.³

It is possible to estimate the resonance absorption fraction from the data in Figs. 1-3. The hot electrons produced by resonance absorption lose energy primarily in collisions with other electrons and by accelerating ions in the corona. The energy loss to corona expansion is observed as fast-ion energy. When collisional losses dominate, the suprathermal electron energy can be estimated from the hard x-ray bremsstrahlung spectrum.¹¹ The treatment by Brysk avoids the difficulty of differentiating an extrapolated experimental spectrum.¹² Brysk's Eq. (7) can be readily evaluated with a Maxwellian electron distribu-

tion, for which the suprathermal electron energy is proportional to the total hard x-ray energy divided by the suprathermal temperature. The hard x-ray energy can be obtained from the data in Figs. 2(a) and 3, and the temperature read directly from Fig. 1. This procedure gives suprathermal electron energy fractions of 10-20% of the incident energy over the full parameter range of the data. If we add the fast-ion energy fraction obtained from the data in Figs. 2(b) and 3, we get an estimate of the total energy in the suprathermal electron energy, and thus the fraction of the incident energy absorbed by resonance absorption. (The model of Refs. 11 and 12 assumes no ion acceleration, so that simply adding these terms is not strictly rigorous.) For the short-pulse data, the totals are 30% at 1.05 μm and 15% at 0.53 μm . For the longer pulses, the totals are 20-25% at 1.05 μm and 15-20% at 0.53 μm . These estimates support the general conclusions that the absorption at 1.05 μm is due primarily to resonance absorption, and that the increased absorption at 0.53 μm is the result of inverse bremsstrahlung. They also suggest that the resonance absorption fraction is somewhat less at the shorter wavelength.

Stimulated Brillouin scattering was not a significant factor in these experiments. Time-resolved measurements of the spectrum of scattered laser light taken during these experiments showed no evidence of stimulated scattering.¹³ Computer simulations of these experiments with use of the one-dimensional fluid hydrodynamic codes obtain reasonable agreement with the data.^{14,15} In one case, Brillouin scattering was not included in the model.¹⁴ Stimulated Brillouin scattering was found to be small in simulations which did include it.¹⁵

In summary, the studies reported here support the expectation that submicron laser light offers important advantages in absorption and hot-electron production compared to 1- μm light. Simulation and experiment indicate that stimulated scattering is not important for the laser and target parameters of these experiments. Additional experiments are required to investigate the wavelength scaling of thermal electron transport and of the hydrodynamic efficiency of the ablation process.

This work was prepared for the U. S. Department of Energy under Contract No. DE-AC08-78OP40030.

¹D. W. Phillion, W. L. Kruer, and V. C. Rupert,

Phys. Rev. Lett. **39**, 1529 (1977).

²D. W. Forslund, J. M. Kindel, and K. Lee, Phys. Rev. Lett. **39**, 284 (1977).

³Kent Estabrook and W. L. Kruer, Phys. Rev. Lett. **40**, 42 (1978).

⁴C. E. Max and K. G. Estabrook, Comments Plasma Phys. Controlled Fusion **5**, 239 (1980).

⁵A. G. M. Maaswinkel, K. Eidmann, and R. Sigel, Phys. Rev. Lett. **42**, 1625 (1979).

⁶E. Fabre, in Proceedings of the International Atomic Energy Agency Technical Committee Meeting on Advances in Inertial Confinement Systems, Osaka, 1980 (unpublished), p. 28.

⁷V. C. Rupert, E. M. Campbell, D. W. Phillion, and F. Ze, in Proceedings of the Tenth Annual Anomalous Absorption Conference, San Francisco, May 1980 (unpublished).

⁸Stephen B. Segall, J. Appl. Phys. **51**, 206 (1980).

⁹C. E. Thomas, Appl. Opt. **14**, 1267 (1975).

¹⁰K. R. Manes *et al.*, J. Opt. Soc. Am. **67**, 717 (1977).

¹¹K. A. Brueckner, Phys. Rev. Lett. **36**, 677 (1976).
Note that the right-hand side of Eq. (3) is too large by a factor of 2.

¹²H. Brysk, Phys. Rev. Lett. **37**, 1242 (1976).

¹³J. A. Tarvin and R. J. Schroeder, KMS Fusion Report No. U-1033 (to be published).

¹⁴R. S. Craxton and R. L. McCrory, University of Rochester, Laboratory for Laser Energetics Report No. 108 (unpublished).

¹⁵D. J. Tanner, D. Mitrovich, R. L. Berger, J. A. Tarvin, and J. Larsen, Bull. Am. Phys. Soc. **25**, 895 (1980), and in Proceedings of the Tenth Annual Anomalous Absorption Conference, San Francisco, May 1980 (unpublished).

Experimental Studies of the Bilateral Ion Blowoff from Laser-Irradiated Thin Plastic Foils

G. D. Tsakiris,^(a) K. Eidmann, R. Petsch, and R. Sigel

Projektgruppe für Laserforschung, Max-Planck-Gesellschaft zur Förderung der Wissenschaften e.V.,

D-8046 Garching, Federal Republic of Germany

(Received 25 September 1980)

Thin plastic foils of various thicknesses (0.13–5.0 μm) were irradiated by iodine-laser pulses with an incident intensity of $4 \times 10^{15} \text{ W cm}^{-2}$. Time-of-flight charge collectors and a Thomson parabola mass spectrometer were used to measure the asymptotic ion velocity distribution at the back and the front (laser) sides of the target. Analysis of these data yielded the ratios of the hot-electron densities and of the hot-electron temperatures at both sides of the foil target. The results disagree with calculations based on classical electron penetration into the foil.

PACS numbers: 52.50.Jm, 52.70.Nc

A major complication of the laser-target interaction problem in laser fusion derives from the fact that a significant fraction of the absorbed laser energy is coupled into a hot-electron component. These hot electrons affect the target behavior in at least two important ways: (i) they create a large electrostatic field in the corona, thus causing fast-ion acceleration and (ii) because of their long range, they may deeply penetrate and preheat the target. These effects may strongly modify the hydrodynamic response of laser-irradiated implosion targets; thin-walled shell targets, for example, have been found to obey a so-called exploding, rather than ablative-ly driven, pusher mode for the energy deposition by fast electrons. Though the subject has been studied for some time in the history of laser fusion,¹ it is still far from quantitative resolution.

For studying the penetration of fast electrons into and through the wall of the target implosion experiments have a certain disadvantage because of their necessarily "closed" spherical geometry.

Experiments in planar geometry using thin-film targets avoid this difficulty since the rear (inner) side becomes accessible. In particular, it then becomes possible to study energy transport through a target by comparing ion emission from both surfaces. Indeed, previous workers have exploited this concept to some extent in studies of reduced thermal conductivity² and, more recently, wavelength dependence of laser-target interaction.³ In this paper we present for the first time detailed ion spectra from the front and rear sides as a function of target thickness. These data allow *quantitative* comparison with continuing theoretical studies of fast electron transport. We shall show on the basis of simple models that the results greatly differ from expectations based on classical electron penetration into the foil. We note that in scope—though not in method—our investigation is similar to recent spectroscopic studies of fast-electron-excited $K\alpha$ radiation from layered targets.⁴

The experiments were carried out with 65-J